ISSN 2278-2540 | DOI: 10.51583/IJLTEMAS | Volume XV, Issue III, March 2026

Microwave-Assisted Oxidation of Cyclohexanecarboxamide by Di-Tertiary-Butyl Chromate in Organic Media: Synthesis and Characterization of Products

Shubhankar Aich[1*] ,Anil Kumar Delta[2]

[1]Assistant Professor, Department of Chemistry, Marwari College Ranchi

[2]Associate Professor, University Department of Chemistry, Ranchi University, Ranchi

[*]Corresponding Author

DOI: https://doi.org/10.51583/IJLTEMAS.2026.150300070

Received: 25 March 2026; Accepted: 30 March 2026; Published: 16 April 2026

ABSTRACT

Microwave irradiation has emerged as a transformative technique in organic synthesis, enabling rapid and energy-efficient chemical transformations. This study investigates the oxidative potential of di-tert-butyl chromate (TBC) in the oxidation of cyclohexanecarboxamide, aiming to develop a faster, sustainable alternative to traditional thermal reflux methods. The oxidation was explored across three distinct organic solvent systems: tetrahydrofuran (THF), 1,4-dioxane, and dichloromethane (DCM). Reaction mixtures were prepared by combining substrate solutions with TBC at standardized stoichiometric ratios. Synthesis was conducted using microwave irradiation for precisely calibrated periods (44–110 s). The resulting coordination complexes were characterized through elemental analysis, Fourier-transform infrared (FTIR) spectroscopy, and thermal analyses, including differential thermal analysis (DTA) and thermogravimetric analysis (TGA). The microwave-assisted approach demonstrated significant kinetic enhancement, reducing reaction times from several hours to under two minutes. Solvent-dielectric synergy was observed, with THF providing the highest efficiency and yield. Characterization confirmed the formation of stable binuclear Cr_2O_3 cores stabilized by a homologous series of dicarboxylate ligands. Mass loss patterns from TGA/DTA further validated the empirical formulations and structural stability of the synthesized complexes. Our findings demonstrate that this microwave-assisted methodology aligns with the principles of green chemistry by minimizing reaction time and energy expenditure. This study provides an efficient and sustainable synthetic route for the oxidation of cyclohexanecarboxamide, offering a versatile template for the development of higher-order chromium (III) coordination frameworks.

Keywords: Microwave-assisted synthesis; Di-tert-butyl chromate; Cyclohexanecarboxamide; Green chemistry; Binuclear chromium complexes.

INTRODUCTION

Microwave-assisted organic synthesis (MAOS)[1–3] and microwave-induced organic reactions (MIOR)[4] have revolutionized organic chemistry by offering sustainable and efficient synthetic approaches for organic compounds. These techniques align with green chemistry[5-8] principles, reduce reaction times, improve yields, and minimize waste generation. The concept of microwave dielectric heating, introduced by Spencer[9] in 1947, was applied to organic synthesis in the pioneering work of Gedye et.al.[10-12] in 1986. Since then, the field has flourished, with over 2000 research articles demonstrating the versatility of microwave-assisted methods in organic synthesis. A comprehensive review by Lindstrom et al[13]. highlighted the advantages of MAOS and MIOR, including significantly reduced reaction times, improved product yields, and minimal waste generation. These techniques are attractive alternatives[14] to conventional heating methods.

In this study, we explored the oxidation of cyclohexanecarboxamide [15] using di-tertiary-butyl chromate[16] (TBC) under microwave irradiation. TBC is a robust and versatile oxidant that has been extensively studied since its

ISSN 2278-2540 | DOI: 10.51583/IJLTEMAS | Volume XV, Issue III, March 2026

introduction by Oppenauer and H. Oberrauch[17] in 1949. The products of cyclohexanecarboxamide have the potential to serve as ligands for the formation of Cr complexes[18] in various oxidation states. Cyclohexanecarboxamide, an alicyclic amide, is a white-to-light-yellow odorless solid. It can act as a precursor for both specialised polymers[19–21] and bioactive molecules[22–25] in agricultural and pharmaceutical chemistry. It is also used for the production of alicyclic amines[26] for further chemical derivatisation it also finds its use in the synthesis of high valent Chromium complexes and mixed ligand[27] coordination compounds. By oxidizing cyclohexanecarboxamide with TBC under microwave irradiation, we synthesized and characterized chromium complexes[28–29] in lower oxidation states. This approach expands the scope of ethyl cyclohexanecarboxamide chemistry and demonstrates the versatility of TBC as an oxidizing agent[30–31].

MATERIALS AND METHODS

Materials and Reagents

All chemicals used in this study were of analytical reagent (A.R.) grade and were used as received without further purification. The primary reagents included cyclohexanecarboxamide (the substrate), chromium (VI) oxide, and tertiary butyl alcohol. The organic solvents used as reaction media were tetrahydrofuran (THF), 1,4-dioxane, and dichloromethane (DCM). Additional reagents for volumetric analysis and purification included acetone, silver nitrate, potassium persulfate, ammonium iron (II) sulfate (Mohr's salt), potassium dichromate, and barium diphenylamine-1-sulfonate.

In-Situ Synthesis of Di-tert-butyl Chromate (TBC)

The oxidant, di-tert-butyl chromate (TBC), was synthesized in situ to ensure maximum oxidation efficiency. A precisely weighed quantity of chromium (VI) oxide was dissolved in 10 mL of tertiary butyl alcohol under constant stirring until a homogenous red-orange solution was obtained, indicating the formation of the chromate ester.

Microwave-Assisted Synthesis and Sample Nomenclature

For each synthesis, 2.0 g of cyclohexanecarboxamide (CHAMIDE) was dissolved in 10 mL of the respective organic solvent (THF, 1,4-dioxane, or DCM) in a rigorously cleaned, desiccated beaker under continuous magnetic stirring at room temperature. The substrate-to-oxidant molar ratios were standardized to 1:1, 2:1, and 3:1. The mixtures were irradiated in a Samsung household microwave oven G-273V (20 L, 2450 MHz, 150 W) for specific durations (44–110 s). Thermometric measurements were recorded immediately before and after irradiation to assess the thermal nature of the reaction. The resulting products were washed with acetone, meticulously dried, and categorized into three series (A, B, and C) based on the solvent medium.

Table 1: Sample Nomenclature and Experimental Parameters

Series Code	Solvent Medium	Substrate Shorthand	Molar Ratios (Sub.: Oxd.)	Sample Labels
Series A	Tetrahydrofuran (THF)	CHAMIDE	1:1,2:1. 3:1	A11, A21, A31
Series B	1,4-Dioxane	CHAMIDE	1:1,2:1. 3:1	B11, B21, B31
Series C	Dichloromethane (DCM)	CHAMIDE	1:1,2:1. 3:1	C11, C21, C31

Note: For final characterization, samples are referred to by combining the Series/Ratio and Substrate code (e.g., A11CHAMIDE).

Analytical and Spectroscopic Characterization

Elemental Analysis and Metal Quantification

The percentage compositions of carbon (C), hydrogen (H), and nitrogen (N) were determined using a EUROVECTOR E-3000 elemental analyser. The chromium (Cr) content was quantified by volumetric titration

ISSN 2278-2540 | DOI: 10.51583/IJLTEMAS | Volume XV, Issue III, March 2026

using potassium persulfate, potassium dichromate, and Mohr's salt. The oxygen (O) content was calculated by difference: O% = 100 - (C% + H% + N% + Cr%). Empirical formulas for all complexes were subsequently deduced from these analytical data.

Instrumental Techniques

- FTIR Spectroscopy: Fourier-transform infrared (FTIR) spectra were recorded on a PerkinElmer spectrometer in the range of 4000–450 cm^{-1} using KBr pellets.
- Thermal Analysis (TG-DTA): Thermogravimetric and differential thermal analyses were performed using a PerkinElmer Diamond TG-DTA system. Samples (approximately 5–10 mg) were heated from ambient temperature to 700°C at a constant ramp rate of 10°C/min under a controlled atmosphere to evaluate mass loss patterns and structural stability.

RESULTS AND DISCUSSION

The exhaustive analytical data in Tables 2–4, integrated with the supplementary FTIR and TG-DTA profiles in the Appendix, provide a rigorous characterization of the Cr–cyclohexanecarboxamide (CHAMIDE) complexes. Systematic evaluation of these physical parameters and elemental compositions facilitates a robust understanding of the complexation mechanism. Consequently, these datasets permit definitive inferences regarding the structural and compositional attributes of the synthesized binuclear chromium (III) frameworks, establishing a comprehensive empirical basis for the proposed chemical formulations of the resultant coordination species.

Table 2: Preliminary product characterisation (Cyclohexanecarboxamide -TBC)

Serial no.	Sample label	Solvent	Subs./ Oxd. Ratio	Microwave Irad. Time (in sec.)	Yield (in gm.)	Colour	Solubility (in water)
1.	A11 CHAMIDE	THF	(1:1) 2g/2g	44	3.12	Dark Brown	Sparingly Soluble
2.	A21 CHAMIDE	THF	(2:1) 2g/1g	60	2.40	Greyish Green	Sparingly Soluble
3.	A31 CHAMIDE	THF	(3:1) 2g/0.67g	72	2.13	Dak Green	Insoluble
4.	B11 CHAMIDE	1,4- Dioxane	(1:1) 2g/2g	75	2.10	Brownish Green	Insoluble
5.	B21 CHAMIDE	1,4- Dioxane	(2:1) 2g/1g	100	1.84	Brownish Green	Insoluble
6.	B31 CHAMIDE	1,4- Dioxane	(3:1) 2g/0.67g	110	1.05	Brownish Green	Insoluble
7.	C11 CHAMIDE	DCM	(1:1) 2g/2g	64	2.55	Greenish Blue	Sparingly Soluble
8.	C21 CHAMIDE	DCM	(2:1) 2g/1g	82	1.86	Greenish Blue	Sparingly Soluble
9.	C31 CHAMIDE	DCM	(3:1) 2g/0.67g	90	1.20	Brownish Green	Insoluble

Table 3: Product formulation– I

Serial No.	Sample No.	Cr%	C%	H%	N%	O%	Empirical Formula
1.	A11CHAMIDE	17.87	14.43	2.06	2.40	63.24	$Cr_2C_7H_{12}NO_{23}$
2.	A21CHAMIDE	19.92	16.09	3.06	2.68	58.25	$Cr_2C_7H_{16}NO_{19}$
3.	A31CHAMIDE	21.94	17.72	3.37	2.95	54.02	$Cr_2C_7H_{16}NO_{16}$
4.	B11CHAMIDE	21.94	17.72	3.37	2.95	54.02	$Cr_2C_7H_{16}NO_{16}$
5.	B21CHAMIDE	23.42	18.92	4.05	3.15	50.46	$Cr_2C_7H_{18}NO_{14}$
6.	B31CHAMIDE	25.49	20.58	3.43	3.43	47.07	$Cr_2C_7H_{14}NO_{12}$
7.	C11CHAMIDE	19.84	16.03	3.43	2.67	58.03	$Cr_2C_7H_{18}NO_{19}$

ISSN 2278-2540 | DOI: 10.51583/IJLTEMAS | Volume XV, Issue III, March 2026

8.	C21CHAMIDE	20.47	16.53	3.54	2.75	56.71	$Cr_2C_7H_{18}NO_{18}$
9.	C31CHAMIDE	24.29	19.63	4.20	3.27	48.61	$Cr_2C_7H_{18}NO_{13}$

Table 4: Product formulation– II

Sl. No.	Sample No.	Empirical Formula	Formulation
1.	A11 CHAMIDE	$Cr_2C_7H_{12}NO_{23}$	Cr_2O_3 (COOH COOH)$_2$ 3CO_2 (H_2O)$_4$ NO_2
2.	A21 CHAMIDE	$Cr_2C_7H_{16}NO_{19}$	Cr_2O_3 ($HOOCCH_2COOH$) (CH_3COOH) (CO_2)$_2$ (H_2O)$_4$ NO_2
3.	A31 CHAMIDE	$Cr_2C_7H_{16}NO_{16}$	Cr_2O_3 ($HOOC(CH_2)_2COOH$) (CH_3COOH) (CO_2) (H_2O)$_3$ NO_2
4.	B11 CHAMIDE	$Cr_2C_7H_{16}NO_{16}$	Cr_2O_3 ($HOOC(CH_2)_2COOH$) (CH_3COOH) (CO_2) (H_2O)$_3$ NO_2
5.	B21 CHAMIDE	$Cr_2C_7H_{18}NO_{14}$	Cr_2O_3 ($HOOC(CH_2)_3COOH$) (CH_3COOH) (H_2O)$_3$ NO_2
6.	B31 CHAMIDE	$Cr_2C_7H_{14}NO_{12}$	Cr_2O_3 ($HOOC(CH_2)_4COOH$) CO (H_2O)$_2$ NO_2
7.	C11 CHAMIDE	$Cr_2C_7H_{18}NO_{19}$	Cr_2O_3 ($HOOCCH_2COOH$) ($HOOCCOOH$) (CH_3COOH) (H_2O)$_4$ NO_2
8.	C21 CHAMIDE	$Cr_2C_7H_{18}NO_{18}$	Cr_2O_3 (HOOC (CH_2) COOH) ($HOOCCOOH$) (CH_3COOH) (H_2O)$_4$ NO
9.	C31 CHAMIDE	$Cr_2C_7H_{18}NO_{13}$	Cr_2O_3 (HOOC (CH_2)$_3$ COOH) (CH_3COOH) (H_2O)$_3$ NO

Synthesis and Preliminary Characterization

A systematic evaluation of the microwave-mediated interactions between cyclohexanecarboxamide and di-tert-butyl chromate (TBC) was conducted, elucidating several critical kinetic and stoichiometric dependencies as delineated below:

- As summarized in Table 2, the microwave methodology facilitated rapid complexation with reaction times ranging from 44 to 110 s. This represents a significant kinetic enhancement over classical thermal methods, which traditionally require several hours of reflux.

- Solvent Influence: The dielectric properties of the solvent significantly modulated the reaction rate and the yield. Tetrahydrofuran (THF) proved to be the most efficient medium, yielding up to 3.12 g (Sample A11) within the shortest irradiation time (44 s). This efficiency is attributed to the optimal dipole moment of THF, which ensures rapid energy transfer during the microwave exposure. In contrast, 1,4-Dioxane and Dichloromethane (DCM) required longer irradiation periods and generally resulted in lower mass recovery.

- Stoichiometric Effects: A clear dependency on the substrate-to-oxidant ratio was observed in this study. The 1:1 ratio consistently provided the highest yields across all solvent systems. As the substrate concentration increased (3:1), a decrease in the yield and a transition to complete water insolubility were observed, suggesting the formation of more hydrophobic or potentially higher-order coordination species.

Elemental Analysis and Empirical Formulation

The elemental compositions (C, H, N, O, and Cr) presented in Table 3 were used to derive the empirical formulas for the synthesized complexes.

ISSN 2278-2540 | DOI: 10.51583/IJLTEMAS | Volume XV, Issue III, March 2026

- Chromium content: The chromium content consistently ranged between 17.87% and 25.49%, increasing as the substrate-to-oxidant ratio shifted from 1:1 to 3:1. This trend indicates that higher substrate concentrations may promote the formation of complexes with a higher relative metal density and a more compact coordination sphere.

- Core Structure: The data consistently indicate a binuclear chromium (III) oxide core (Cr_2O_3). This suggests that during the microwave-assisted process, Cr (VI) in TBC undergoes partial reduction and subsequent condensation to form a stable oxo-bridged binuclear framework.

Proposed Structural Formulation and Ligand Fragmentation

The structural formulations detailed in Table 4 provide deep insights into the oxidative role of TBC. The cyclohexanecarboxamide moiety undergoes systematic oxidative ring-opening and fragmentation reaction.

- Oxidative Cleavage: The identification of various dicarboxylate ligands, including oxalic, malonic, succinic, glutaric, and adipic acids, within the coordination sphere suggests that TBC facilitates the cleavage of the cyclohexane ring at different positions depending on the reaction conditions.

- Coordination Environment: The Cr_2O_3 core is further stabilized by auxiliary ligands, including acetate groups (likely derived from TBC degradation or oxidative byproducts), nitro groups (NO_2), and neutral molecules such as CO_2 and H_2O.

- Solvent-Dependent Coordination: Notably, the choice of solvent influenced the specific dicarboxylate formed. For instance, THF systems (A-series) yielded oxalate, malonate, and succinate fragments, whereas 1,4-Dioxane (B-series) favoured longer-chain fragments such as glutarate and adipate. This indicates that the solvent medium plays a role in stabilizing specific transition states during the oxidative degradation of carboxamides.

Physical Properties and Stability

The transition in product colour from dark brown to greenish-blue and dark green is indicative of d-d transitions within the chromium centres, consistent with the coordination of different carboxylate ligands. The shift in solubility from sparingly soluble to insoluble as the organic fraction increases suggests that the complexes become more polymeric or less polar as the chain length of the coordinated dicarboxylate increases.

Reproducibility Details

The yields showed a solvent-dependent range with high reproducibility within the "High" and "Low" efficiency bands.

- Overall Yield Range: 1.05 g to 3.12 g.

- Mean Yield by Series:

- THF (A-Series): 2.55 g ± 0.51 g

- DCM (C-Series): 1.87 g ± 0.68 g

- 1,4-Dioxane (B-Series): 1.66 g ± 0.55 g

- Yield Reproducibility: The 1:1 ratio consistently delivered the highest mass recovery across all solvents (range: 2.10–3.12 g), whereas the 3:1 ratio consistently produced the lowest (range: 1.05–2.13 g).

ISSN 2278-2540 | DOI: 10.51583/IJLTEMAS | Volume XV, Issue III, March 2026

- The data suggest that the THF series (A) is the most reproducible for high-yield applications (yield > 2.0 g), while the 1,4-Dioxane series (B) provides the most consistent colour and solubility profile (Uniformly Brownish Green and Insoluble), regardless of the stoichiometric ratio used.

CONCLUSION

The microwave-assisted synthesis of chromium-coordinated complexes yielded several pivotal conclusions regarding reaction efficiency, structural formation, and methodological innovation.

Core Research Findings

- Kinetic Acceleration: The application of microwave radiation represents a paradigm shift in synthesis time, achieving complexation within 44–110 s of microwave exposure. This offers a dramatic reduction in energy consumption compared to the multi-hour reflux cycles required by traditional thermal methods.

- Dielectric and Solute Synergy: The high efficiency of THF (yielding 3.12 g) highlights the importance of dielectric coupling in the DES. Interestingly, the success in low-absorbing solvents like 1,4-Dioxane suggests a "molecular radiator" effect, where polar reactants directly absorb electromagnetic energy to drive the reaction.

- Structural Integrity: Regardless of the solvent used, the process consistently produced a stable binuclear Cr_2O_3 core. This framework is stabilized by a series of dicarboxylate ligands (ranging from Oxalic to Adipic acid) produced through the systematic oxidative ring-opening of the cyclohexane precursor.

- Stoichiometric Influence: Experimental data confirmed that a 1:1 substrate-to-oxidant ratio was optimal for yield. Increasing this to a 3:1 ratio result in a higher metal density and structural shift toward insoluble, potentially polymeric coordination environments.

Scientific Novelty

The primary innovation of this study is the discovery of a solvent-directed oxidative fragmentation reaction. This demonstrates that the organic medium does more than just regulate the reaction rate; it actively determines which dicarboxylate fragments are stabilized within the coordination sphere. Furthermore, using di-tert-butyl chromate (TBC) as a dual-purpose reagent, both an oxidant and a source of auxiliary ligands, establishes a streamlined "one-pot" synthetic route to complex binuclear structures that are typically inaccessible via conventional thermal pathways.

Future Strategic Directions

To further advance this field, the following research pathways are proposed:

- Mechanistic Investigations: In-situ UV-Vis or IR spectroscopy was employed to observe the real-time reduction of Cr (VI) to Cr (III) and the sequential stages of ring cleavage.

- Catalytic Exploration: Assessing the potential of these binuclear complexes as catalysts in selective oxidation or as precursors for advanced mixed-metal oxide materials.

- Magneto chemical Analysis: Studying the magnetic exchange interactions across the oxo-bridged chromium centres to evaluate their potential in molecular magnetism.

Crystallographic Validation: Single-crystal X-ray diffraction was performed to map the spatial orientation of the coordinated ligands, including auxiliary H_2O and CO_2 molecules

ISSN 2278-2540 | DOI: 10.51583/IJLTEMAS | Volume XV, Issue III, March 2026

ACKNOWLEDGMENTS

The authors acknowledge the cooperation and assistance provided by BIT Mesra and SAIF Lucknow, which facilitated the testing and analysis of the samples.

Authors Contributions:

[Author 1]: Conceptualization, methodology, software, validation, formal analysis, investigation, resources, data curation, writing (original draft), and funding acquisition.
[Author 2]: Conceptualization, methodology, visualization, supervision, validation, formal analysis, investigation, resources, data curation, writing (review and editing), project administration.

Funding:

The researchers did not receive any external funding for this study.

Conflict of interest:

The authors declare no conflicts of interest.

REFERENCES

1. Kappe, C. O. "Microwave-Assisted Chemistry." In "Microwave-Assisted Organic Synthesis," pp. 1-19. Springer, 2013.
2. De la Hoz, A., et al. (2011). Microwave-Assisted Organic Synthesis: A Critical Review. Tetrahedron, 67(2), 283-303.
3. Swami, S., et al. (2025). "Recent advances in microwave-assisted synthesis: a green approach toward sustainable development." RSC Adv., 15, 2361.
4. Singh, M. S., & Singh, A. K. (2019). Microwave-Induced Organic Reactions: A Review. Journal of Chemical Research, 43(10), 557-562.
5. The twelve principles of Green Chemistry' United States Environmental Protection Agency. 2006 Retrieved.
6. Lahoz, Antonio De, Diaz-Ortiz, Angel and Prieto, Pilar, Microwave assisted green organic synthesis in alternative energy sources for green chemistry, 2016 pp. 1-33.
7. Sajini, T., & Joseph, J. (2025). "Microwave-assisted synthesis of nanomaterials: a green chemistry perspective and sustainability assessment." RSC Sustainability, 3, 4911-4935. [DOI: 10.1039/D5SU00584A]
8. Banerjee, S., et al. (2025). "Revolutionizing organic synthesis through green chemistry: metal-free, bio-based, and microwave-assisted methods." Front. Chem., 13. [DOI: 10.3389/fchem.2025.1656935]
9. Spencer, P., "Method of Treating Foodstuffs," US Patent 2,495,429, 1950.
10. Gedye, R., Smith, F., Westaway, K., Ali, H., Baldisera, L., Laberge, L., & Rousell, J. (1986). The use of microwave ovens for rapid organic synthesis. Tetrahedron Letters, 27(3), 279-282.
11. Gedye, R. N., & Wei, J. B. (1998). Microwave-assisted organic synthesis: A review. Canadian Journal of Chemistry, 76(5), 525-532.
12. Gedye, R. N., & Rank, W. (1999). Microwave-assisted organic synthesis in solvent-free conditions. Journal of Chemical Research, Synopses, (10), 542-543.
13. Lindstrom, P., Tierney, J., Wathey, B. and Westman, J. "Microwave Assisted Organic Synthesis-a Review," Tetrahedron, vol. 57, no. 45, pp. 9225-9283, 2001.
14. Katre, Sangita; Study of oxidation of chromic acid with chromium complexes by classical and green approach; Der Chemica Sinicia,2014, 5 (6) Pelagia Research Library, pp 48-50.
15. Cyclohexanecarboxamide – Wikidata https://share.google/ACf6pecKFWFbiA2Qg.
16. Wheeler, J.M., "Ditertiary Butyl Chromate: A Versatile Oxidant," Journal of Chemical Research, vol. 2001, no. 10, pp. 432-433, 2001.

ISSN 2278-2540 | DOI: 10.51583/IJLTEMAS | Volume XV, Issue III, March 2026

17. Oppenaur, R.V. and Oberrauch, H. "Oxidation of Amines with Di-tert-butyl Chromate," Journal of the American Chemical Society, vol. 71, no. 10, pp. 3421-3424, 1949.
18. Nair, A., et al. (2025). "Role of Biomolecules in Modifying the Structural and Optical Properties of Chromium (VI) Complexes." IJSRCP, 5(2), 009-018.
19. Blomenhofer, M.; Ganzleben, S.; Hanft, D.; Schmidt, H. W. "Cyclohexanecarboxamides as Highly Efficient Nucleating Agents for Polypropylene." Macromolecules, 2005, 38(9), 3688–3695.
20. Kristiansen, M.; Tervoort, T.; Smith, P. "Synergistic Nucleation of Poly(propylene) by Cyclohexanecarboxamide Derivatives." Polymer, 2003, 44(19), 5885–5891.
21. Mohammadi, A. Z.; Garmabi, H. "Effect of Cyclohexanecarboxamide Derivatives on the Crystallization Kinetics and Morphology of Polypropylene." Journal of Applied Polymer Science, 2011, 121(4), 2322–2330.
22. Scherer, O.; Knauf, W. "N-Cyclohexylcarboxamides: A New Class of Systemic Fungicides." Pesticide Science, 1974, 5(2), 155–160.
23. Smith, P. J.; Taylor, R. J.; Jones, A. M. "Cyclohexyl-substituted Amides as Hydrophobic Mimics in Protease Inhibition." Bioorganic & Medicinal Chemistry Letters, 1996, 6(12), 1483–1488.
24. Canceill, J.; Gabard, J.; Schierer, O. "Synthesis and Anticonvulsant Activity of Some Cyclohexanecarboxamide Derivatives." European Journal of Medicinal Chemistry, 1980, 15(3), 221–225.
25. Paprocka, R., et al. (2025). "Synthesis, Evaluation of Biological Activity, and Structure–Activity Relationships of New Amidrazone Derivatives Containing Cyclohexane Systems." Molecules, 30(8), 1853
26. Wallis, E. S.; Lane, J. F. "The Hofmann Rearrangement." Organic Reactions, 1946, 3, 267–306.
27. Sigel, H.; Martin, R. B. "Coordinating Properties of the Amide Group." Chemical Reviews, 1982, 82(4), 385–426.
28. Steiman, T. J., & Uyeda, C. (2015). "Reagents for Reductive Transition Metal Catalysis." Chemical Science, 6, 2327–2337.
29. Zeng, X. (2013). "Recent Advances in Chromium-Catalyzed Carbon–Carbon Bond-Forming Reactions." Chemical Society Reviews, 42(13), 5658–5671.
30. Katre, Sangita and Pandey, H.O. A Green approach to oxidation of succinic acid by chromium (VI) based complexes functioning as oxidant in International Journal of green chemistry and Bioprocess 2013 3(3) pp.3032.
31. Katre, Sangita D. Recent Advances in the Oxidation Reactions of Organic Compounds using Chromium (VI) Reagents in Res.J.Chem.Environ. Vol. 24 (1) January (2020).

ISSN 2278-2540 | DOI: 10.51583/IJLTEMAS | Volume XV, Issue III, March 2026

Appendix

Supplementary Spectroscopic and Thermal Data

Fig. (i) FTIR Spectrum of A11 CHAMIDE

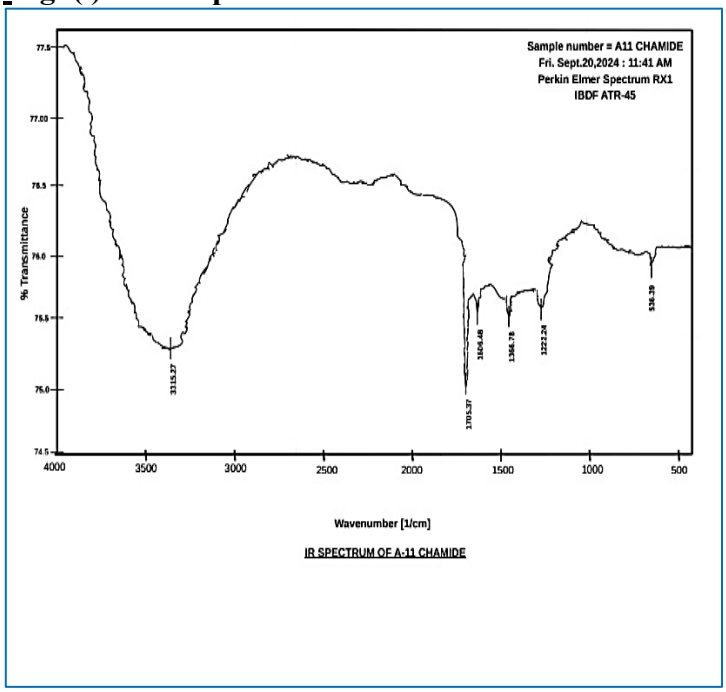

Table (i): IR absorption peaks of A11 CHAMIDE

Peaks (1/cm)	Nature of Peak	Groups Assigned
3315.27	Broad, Strong	O-H stretching
1705.37	Sharp, Strong	C=O stretching
1606.48	Sharp, Strong	N-O asymmetric stretching
1366.78	Sharp, Medium	N-O symmetric stretching
1222.24	Sharp, Medium	C-O stretching
536.39	Broad, Weak	Cr-O stretching

Fig. (ii) FTIR Spectrum of A21 CHAMIDE

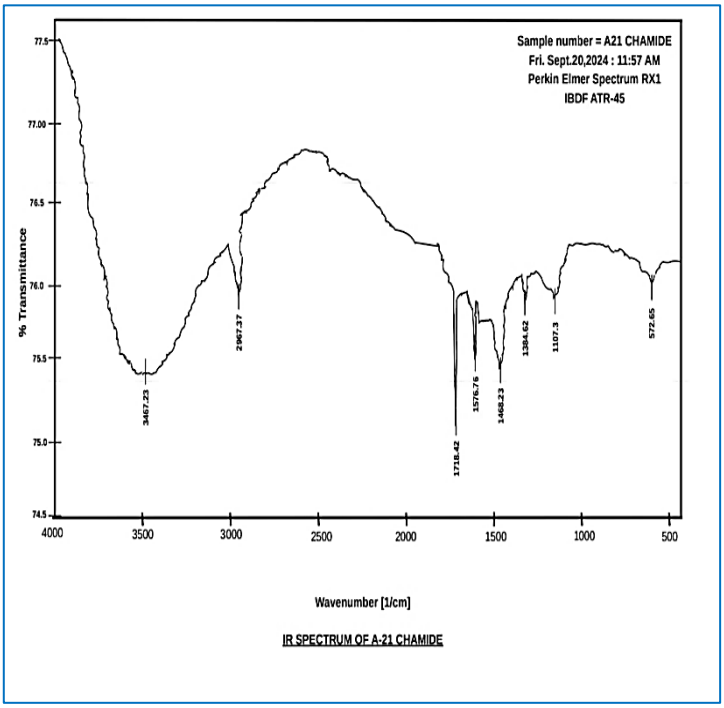

Table (ii): IR absorption peaks of A21 CHAMIDE

Peaks (1/cm)	Nature of Peak	Groups Assigned
3467.23	Broad, Strong	O-H stretching
2967.37	Sharp, Medium	C-H stretching
1718.42	Sharp, Strong	C=O stretching
1576.76	Sharp, Strong	N-O asymmetric stretching
1468.23	Sharp, Strong	O-H in plane bending
1384.82	Sharp, Medium	N-O symmetric stretching
1207.30	Sharp, Medium	C-O stretching
572.65	Broad, Weak	Cr-O stretching

Fig. (iii) FTIR Spectrum of A31 CHAMIDE

ISSN 2278-2540 | DOI: 10.51583/IJLTEMAS | Volume XV, Issue III, March 2026

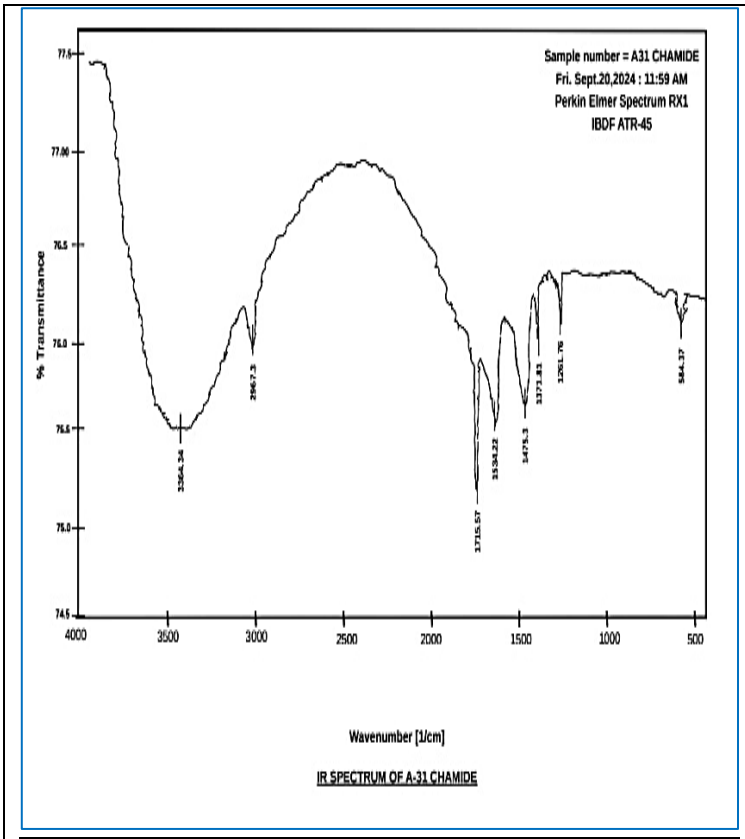

Table (iii): IR absorption peaks of A31 CHAMIDE

Peaks (1/cm)	Nature of Peak	Groups Assigned
3364.34	Broad, Strong	O-H stretching
2967.30	Sharp, Medium	C-H stretching
1715.57	Sharp, Strong	C=O stretching
1534.22	Sharp, Strong	N-O asymmetric stretching
1475.30	Sharp, Strong	O-H in plane bending
1371.81	Sharp, Medium	N-O symmetric stretching
1261.76	Sharp, Medium	C-O stretching
584.37	Broad, Weak	Cr-O stretching

Fig. (iv) FTIR Spectrum of B11 CHAMIDE

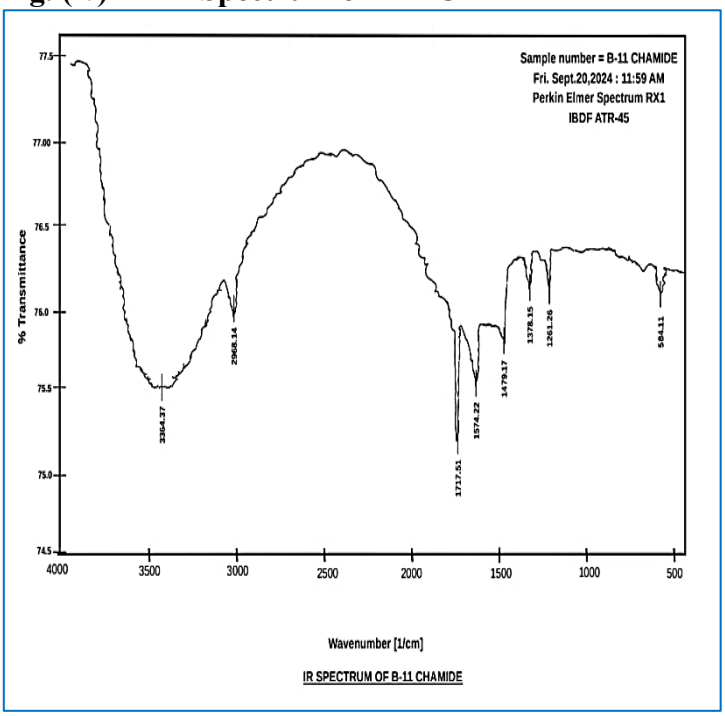

Table (iv): IR absorption peaks of B11 CHAMIDE

Peaks (1/cm)	Nature of Peak	Groups Assigned
3364.37	Broad, Strong	O-H stretching
2968.14	Sharp, Medium	C-H stretching
1717.51	Sharp, Strong	C=O stretching
1574.22	Sharp, Strong	N-O asymmetric stretching
1479.17	Sharp, Strong	O-H in plane bending
1378.15	Sharp, Medium	N-O symmetric stretching
1261.26	Sharp, Medium	C-O stretching
584.11	Broad, Weak	Cr-O stretching

Fig. (v) FTIR Spectrum of B21 CHAMIDE

Table (v): IR absorption peaks of B21 CHAMIDE

ISSN 2278-2540 | DOI: 10.51583/IJLTEMAS | Volume XV, Issue III, March 2026

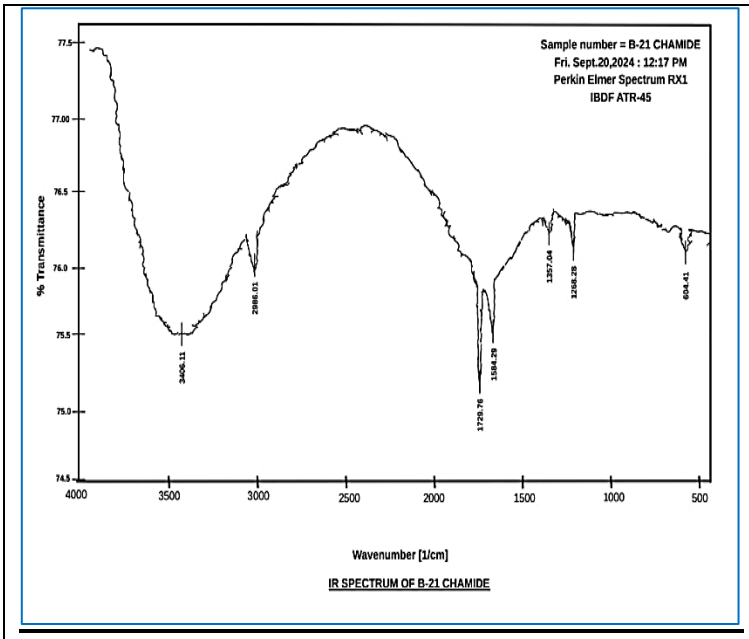

Peaks (1/cm)	Nature of Peak	Groups Assigned
3406.11	Broad, Strong	O-H stretching
2986.01	Sharp, Medium	C-H stretching
1729.76	Sharp, Strong	C=O stretching
1584.29	Sharp, Strong	N-O asymmetric stretching
1357.04	Sharp, Medium	N-O symmetric stretching
1268.28	Sharp, Weak	C-O stretching
604.41	Broad, Weak	Cr-O stretching

Fig. (vi) FTIR Spectrum of B31 CHAMIDE

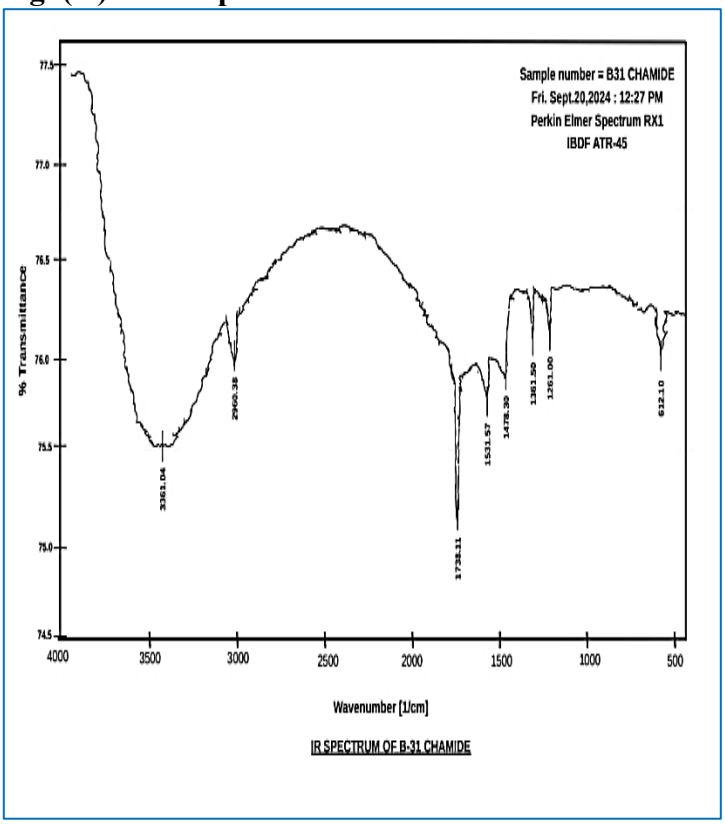

Table (vi): IR absorption peaks of B31 CHAMIDE

Peaks (1/cm)	Nature of Peak	Groups Assigned
3361.04	Broad, Strong	O-H stretching
2960.38	Sharp, Medium	C-H stretching
1738.11	Sharp, Strong	C=O stretching
1531.57	Sharp, Strong	N-O asymmetric stretching
1478.30	Sharp, Strong	O-H in plane bending
1361.50	Sharp, Medium	N-O symmetric stretching
1261.00	Sharp, Medium	C-O stretching
612.10	Broad, Weak	Cr-O stretching

ISSN 2278-2540 | DOI: 10.51583/IJLTEMAS | Volume XV, Issue III, March 2026

Fig. (vii) FTIR Spectrum of C11 CHAMIDE

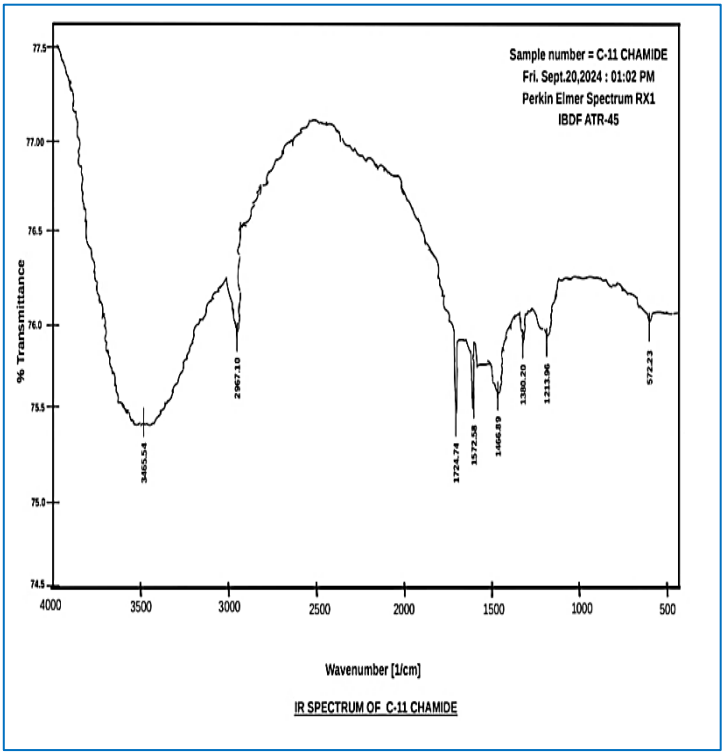

Table (vii): IR absorption peaks of C11 CHAMIDE

Peaks (1/cm)	Nature of Peak	Groups Assigned
3465.54	Broad, Strong	O-H stretching
2967.10	Sharp, Medium	C-H stretching
1724.74	Sharp, Strong	C=O stretching
1572.58	Sharp, Strong	N-O asymmetric stretching
1466.89	Sharp, Strong	O-H in plane bending/C-H scissoring
1380.20	Sharp, Medium	N-O symmetric stretching
1213.96	Sharp, Medium	C-O stretching
572.23	Broad, Weak	Cr-O stretching

Fig. (viii) FTIR Spectrum of C21 CHAMIDE

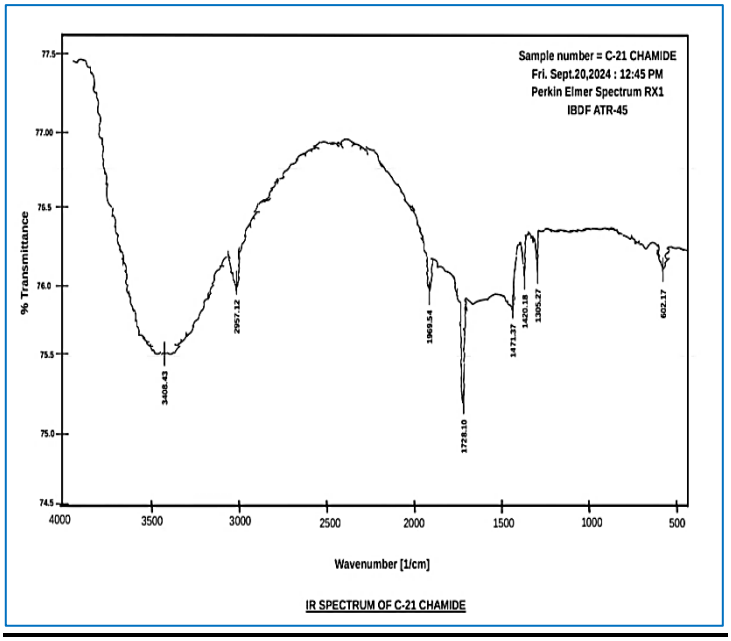

Table (viii): IR absorption peaks of C21 CHAMIDE

Peaks (1/cm)	Nature of Peak	Groups Assigned
3408.43	Broad, Strong	O-H stretching
2957.12	Sharp, Medium	C-H stretching
1969.54	Sharp, Medium	N-O stretching
1728.10	Sharp, Strong	C=O stretching
1471.37	Sharp Weak	C-H scissoring of CH_2group
1420.18	Sharp, Medium	C-O asymmetric stretching
1305.27	Sharp, Weak	C-O stretching
602.17	Broad, Weak	Cr-O stretching

ISSN 2278-2540 | DOI: 10.51583/IJLTEMAS | Volume XV, Issue III, March 2026

Fig. (ix) FTIR Spectrum of C31 CHAMIDE

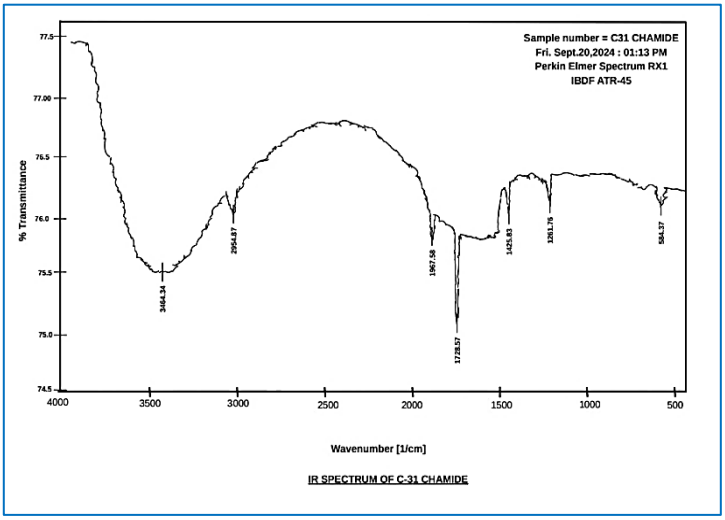

Table (ix): IR absorption peaks of C31 CHAMIDE

Peaks (1/cm)	Nature of Peak	Groups Assigned
3464.34	Broad, Strong	O-H stretching
2954.87	Sharp, Medium	C-H stretching
1967.58	Sharp, Strong	N-O stretching
1728.57	Sharp, Strong	C=O stretching
1425.83	Sharp, Medium	C-O asymmetric stretching
1261.76	Sharp, Weak	C-O stretching
584.37	Broad, Weak	Cr-O stretching

Fig (x) TGA OF A11 CHAMIDE

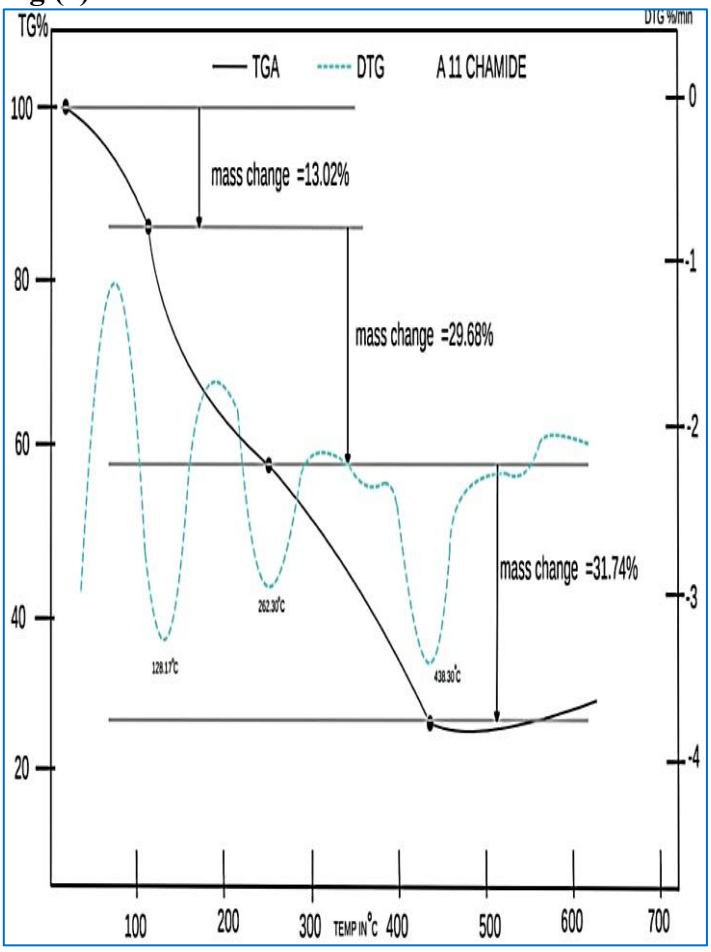

➢ Sample A11 CHAMIDE, with the empirical formula $Cr_2C_7H_{12}NO_{23}$, showed a mass loss of 13.02% (theoretical 12.37%), which was due to the loss of H_2O in the temperature range (30°-150° C). The TGA curve showed the loss of CO_2 and NO_2 between 150°-300° C temperature with a mass loss of 29.68% (theoretical 30.58%) and the loss of (COOH COOH) between 300°-700 °C temperature with a mass loss of 31.74% (theoretical 30.92%). The residual part was chromium and its oxides, which was 25.56% (theoretical 26.13%) [Fig (x)].

➢ In accordance with the elemental analysis, FTIR spectral data, and thermal analysis of A11 CHAMIDE, the proposed formulation of A11 CHAMIDE is Cr_2O_3 (COOH COOH)$_2$ $3CO_2$ $(H_2O)_4$ NO_2.

Fig (xi)TGA OF A21 CHAMIDE

• Sample A21 CHAMIDE having empirical formula $Cr_2C_7H_{16}NO_{19}$ showed mass

ISSN 2278-2540 | DOI: 10.51583/IJLTEMAS | Volume XV, Issue III, March 2026

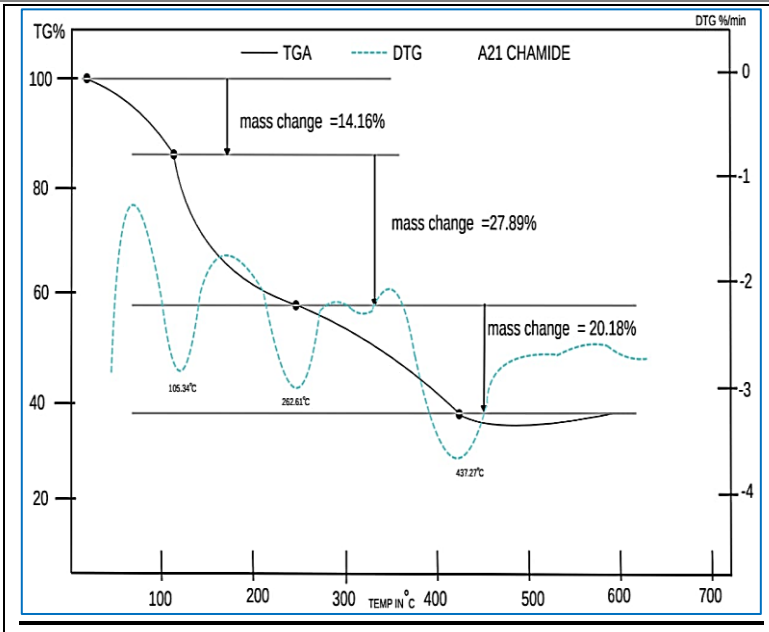

loss of 14.16% (theoretical 13.79%) which was due to loss of H_2O in the temperature range (30°-150° C). The TGA curve showed the loss of CO_2, CH_3COOH and NO_2 in between 150°-300° C temperature with the mass loss of 27.89% (theoretical 28.73%) and loss of HOOC CH_2 COOH in between 300-700°C temperature with the mass loss of 20.18% (theoretical 19.92%). The residual part was Chromium and its oxides which was 37.77% (theoretical 37.56%) [Fig. (xi)].

- In accordance with elemental analysis, FTIR spectral and thermal analysis of A21 CHAMIDE, the proposed formulation of A21 CHAMIDE is Cr_2O_3 $(HOOCCH_2COOH)$ (CH_3COOH) $(CO_2)_2$ $(H_2O)_4$ NO_2

Fig (xii)TGA OF A31 CHAMIDE

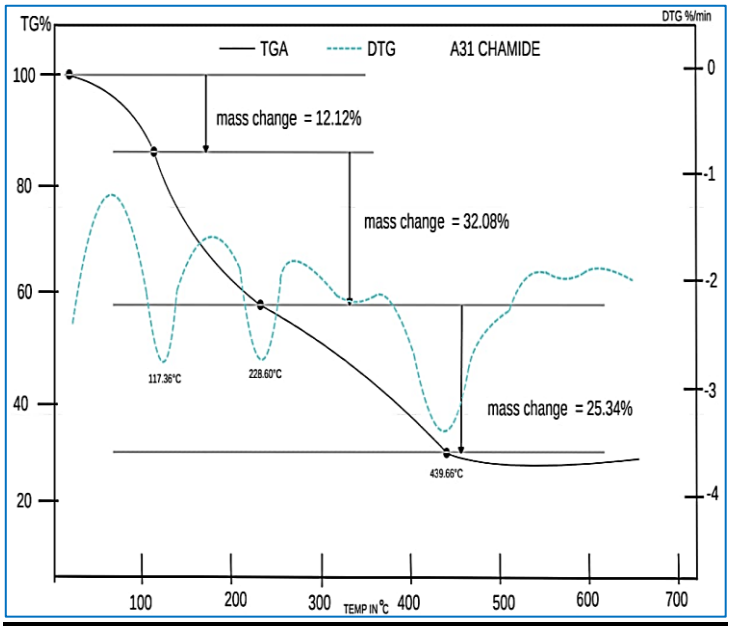

- Sample A31 CHAMIDE with empirical formula $Cr_2C_7H_{16}NO_{16}$ showed mass loss of 12.12% (theoretical 11.39%), which was due to the loss of H_2O in the temperature range (30°-150° C). The TGA curve showed the loss of CH_3COOH, CO_2, and NO_2 between 150°-300° C temperature with a mass loss of 32.08% (theoretical 31.64%) and the loss of $HOOC(CH_2)_2COOH$ between 300-700°C temperature with a mass loss of 25.34% (theoretical 24.89%). The residual part was chromium and its oxides, which was 30.46% (theoretical 32.08%) [Fig (xii)]
- Based on elemental analysis, FTIR spectral data, and thermal analysis of A31 CHAMIDE, the proposed formulation of A31 CHAMIDE is $Cr_2O_3(HOOC(CH_2)_2COOH)$ (CH_3COOH) (CO_2) $(H_2O)_3$ NO_2.

ISSN 2278-2540 | DOI: 10.51583/IJLTEMAS | Volume XV, Issue III, March 2026

Fig (xiii)TGA OF B11 CHAMIDE

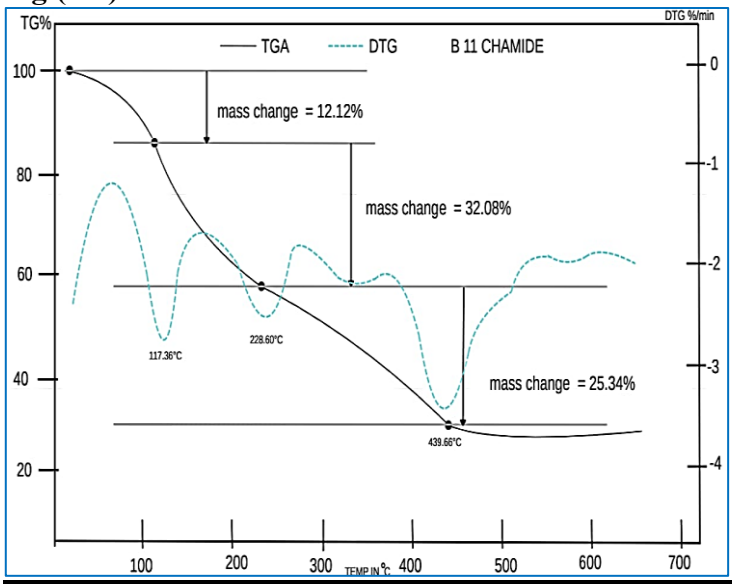

- Sample B11 CHAMIDE with the empirical formula $Cr_2C_7H_{16}NO_{16}$ showed a mass loss of 12.12% (theoretical 11.39%), which was due to the loss of H_2O in the temperature range (30°-150° C). The TGA curve showed the loss of CH_3COOH, CO_2, and NO_2 between 150°-300° C temperature with a mass loss of 32.08% (theoretical 31.64%) and the loss of $HOOC(CH_2)_2COOH$ between 300-700°C temperature with a mass loss of 25.34% (theoretical 24.89%). The residual part was chromium and its oxides, which was 30.46% (theoretical 32.08%) [Fig (xiii)]
- Based on the elemental analysis and FTIR spectral thermal analysis of B11 CHAMIDE, the proposed formulation of B11 CHAMIDE is $Cr_2O_3(HOOC(CH_2)_2COOH)$ (CH_3COOH) (CO_2) $(H_2O)_3$ NO_2.

Fig (xiv)TGA OF B21 CHAMIDE

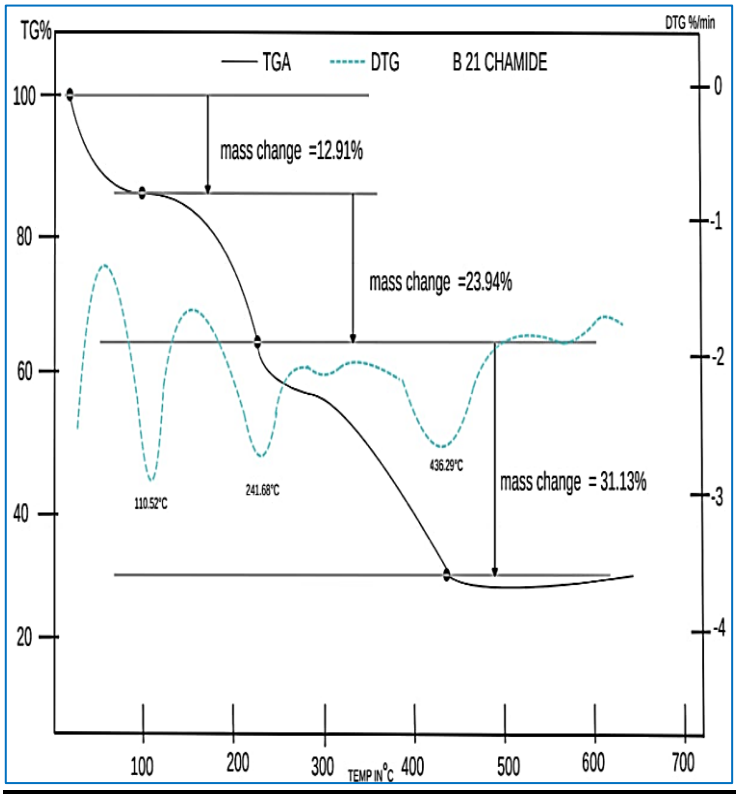

- The sample B21 CHAMIDE having empirical formula $Cr_2C_7H_{18}NO_{14}$ showed mass loss of 12.91% (theoretical 12.16%) which was due to loss of H_2O in the temperature range (30°-150° C). The TGA curve showed the loss of NO_2 and CH_3COOH in between 150°-300° C temperature with the mass loss of 23.94% (theoretical 23.87%) and loss of $HOOC(CH_2)_3COOH$ in between 300°-700°C temperature with the mass loss of 31.13% (theoretical 29.73 %). The residual part is Chromium and its oxides which was 32.02% (theoretical 34.24%) [Fig (xiv)]

- In accordance with elemental analysis, FTIR analysis and thermal analysis of B21 CHAMIDE, the proposed formulation of B21 CHAMIDE is, spectral and thermal analysis was Cr_2O_3 $(HOOC(CH_2)_3COOH)$ (CH_3COOH) $(H_2O)_3$ NO_2

ISSN 2278-2540 | DOI: 10.51583/IJLTEMAS | Volume XV, Issue III, March 2026

Fig (xv)TGA OF B31 CHAMIDE

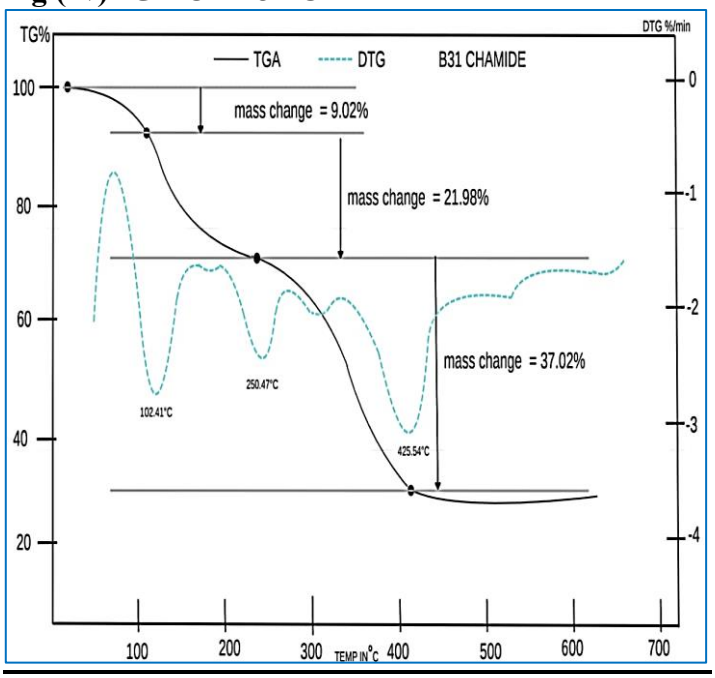

➢ Sample B31 CHAMIDE with empirical formula $Cr_2C_7H_{14}NO_{12}$ showed mass loss of 9.02% (theoretical 8.82%), which is due to the loss of H_2O in the temperature range (30°-150° C). The TGA curve showed the loss of NO_2 and CO in the 150°-300° C temperature with a mass loss of 21.98% (theoretical 22.05%) and the loss of $COOH(CH_2)_4COOH$ in the 300°-700 °C temperature range with a mass loss of 37.02% (theoretical 35.78%). The residual part was chromium and its oxides, which was 31.98% (theoretical 33.35%) [Fig(xv)].

➢ In accordance with the elemental analysis, FTIR spectral data, and thermal analysis of B31 CHAMIDE, the proposed formulation of B31 CHAMIDE was Cr_2O_3 $(HOOC(CH_2)_4COOH)$ CO $(H_2O)_2$ NO_2.

Fig (xvi)TGA OF C11 CHAMIDE

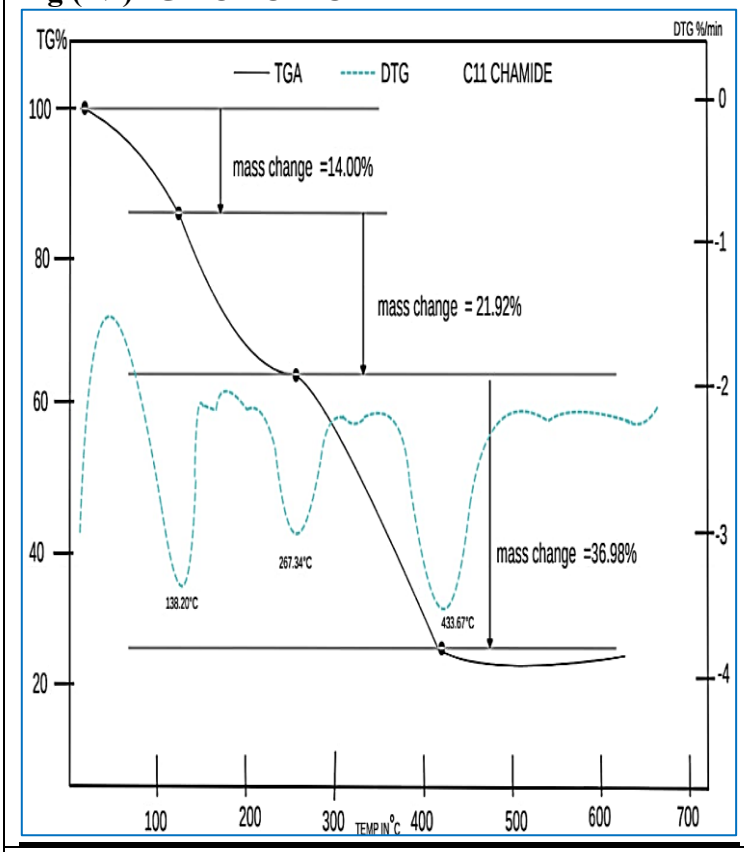

➢ Sample C11 CHAMIDE, with the empirical formula $Cr_2C_7H_{18}NO_{19}$, showed a mass loss of 14.00% (theoretical 13.74%), which was due to the loss of H_2O in the temperature range (30°-150° C). The TGA curve showed the loss of CH_3COOH and NO_2 between 150°-300° C with a mass loss of 21.92% (theoretical 20.23%) and the loss of $HOOCCH_2COOH$ and HOOCCOOH between 300-700°C temperature with a mass loss of 36.98% (theoretical 37.02%). The residual part was chromium and its oxides, which was 27.10% (theoretical 29.02%) [Fig (xvi)]

➢ In accordance with the elemental analysis and FTIR spectral thermal analysis of C11 CHAMIDE, the proposed formulation of C11 CHAMIDE was $Cr_2O_3(HOOC(CH_2)$ COOH) (CH_3COOH) $(HOOCCOOH$ $(H_2O)_4$ NO_2.

Fig (xvii)TGA OF C21 CHAMIDE

➢ Sample C21 CHAMIDE, with the empirical formula $Cr_2C_7H_{18}NO_{18}$, showed a mass loss of 14.81% (theoretical 14.17%), which was

ISSN 2278-2540 | DOI: 10.51583/IJLTEMAS | Volume XV, Issue III, March 2026

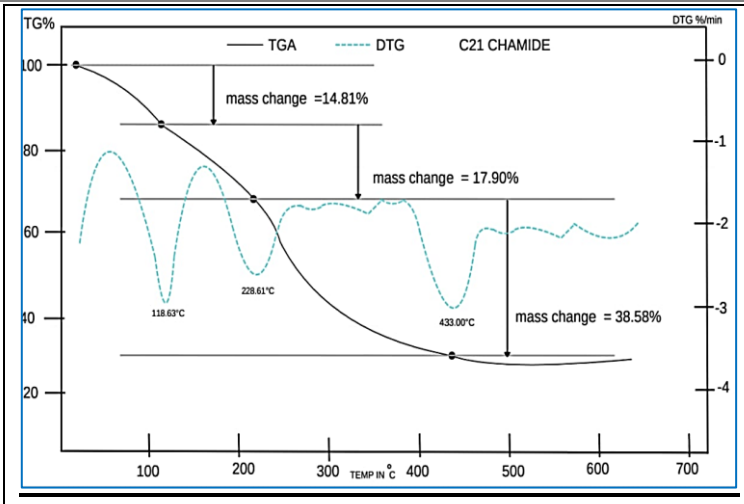

due to the loss of H_2O in the temperature range (30°-150° C). The TGA curve showed the loss of NO and CH_3COOH between 150°-300° C temperature with a mass loss of 17.90% (theoretical 17.71%) and the loss of HOOC (CH_2) COOH and HOOCCOOH between 300°-700°C temperature with a mass loss of 38.58% (theoretical 38.18%). The residual part was chromium and its oxides, which was 28.71% (theoretical 29.94%) [Fig(xvii)].

- In accordance with elemental analysis, FTIR analysis and thermal analysis of C21 CHAMIDE, the proposed formulation of C21 CHAMIDE was, spectral and thermal analysis is Cr_2O_3 (HOOC (CH_2) COOH) (HOOCCOOH) (CH_3COOH) $(H_2O)_4$ NO.

Fig (xviii)TGA OF C31 CHAMIDE

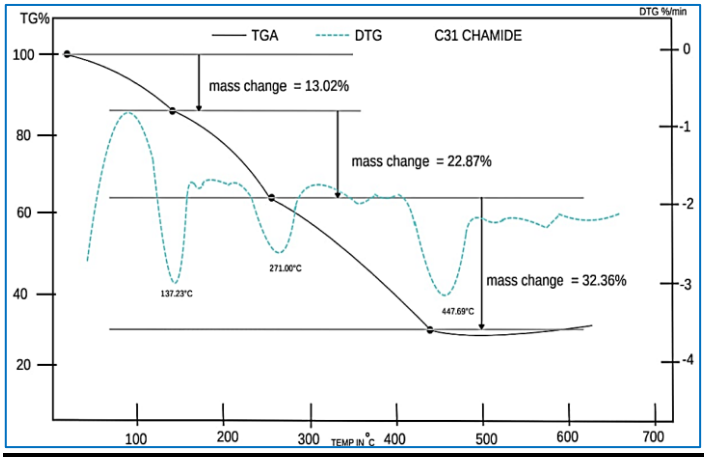

- Sample C31 CHAMIDE with empirical formula $Cr_2C_7H_{18}NO_{13}$ showed mass loss of 13.02% (theoretical 12.61%), which was due to the loss of H_2O in the temperature range (30°-150° C). The TGA curve showed the loss of NO and CH3COOH between 150°-300° C temperature with a mass loss of 22.87% (theoretical 21.02%) and the loss of $COOH(CH_2)_4COOH$ between 300°-700 °C temperature with a mass loss of 32.36% (theoretical 30.84%). The residual part was chromium and its oxides, which was 31.75% (theoretical 35.53%) [Fig (xviii)].
- In accordance with the elemental analysis, FTIR spectral data, and thermal analysis of C31 CHAMIDE, the proposed formulation of C31 CHAMIDE was Cr_2O_3 (HOOC $(CH_2)_3$ COOH) (CH_3COOH) $(H_2O)_3$ NO.